PHYSICAL REVIEW B **81**, 121308(R) (2010)

Kondo-enhanced Andreev transport in single self-assembled InAs quantum dots contacted with normal and superconducting leads

R. S. Deacon,[1,*] Y. Tanaka,[2] A. Oiwa,[1,3,4] R. Sakano,[1] K. Yoshida,[3] K. Shibata,[5] K. Hirakawa,[4,5,6] and S. Tarucha[1,3,6,7]
[1]*Department of Applied Physics, The University of Tokyo, 7-3-1 Hongo, Bunkyo-ku 113-8656, Japan*
[2]*RIKEN, Condensed Matter Theory Laboratory, Wako, Saitama 351-0198, Japan*
[3]*ICORP JST, 3-1 Wakamiya, Morinosato, Atsugi-shi, Kanagawa 243-0198, Japan*
[4]*JST CREST, 4-1-8 Hon-cho, Kawaguchi-shi, Saitama 332-0012, Japan*
[5]*Institute of Industrial Science, The University of Tokyo, 4-6-1 Komaba, Meguro-ku, Tokyo 153-8505, Japan*
[6]*INQIE, The University of Tokyo, 4-6-1 Komaba, Meguro-ku, Tokyo 153-8505, Japan*
[7]*QPEC, The University of Tokyo, 7-3-1 Hongo, Bunkyo-ku 113-8656, Japan*
(Received 20 January 2010; published 25 March 2010)

We study transport in self-assembled InAs quantum dots contacted with one superconducting and one normal-metal electrode. Low bias transport is dominated by Andreev processes which are sensitive to local correlations such as electron-electron interaction and the Kondo effect. We identify that, for appropriate tunnel coupling with normal and superconducting leads, Andreev transport is enhanced by the Kondo effect and that the Kondo temperature is reduced relative to the normal state due to lack of low-energy excitations with the superconducting lead.

DOI: 10.1103/PhysRevB.81.121308 PACS number(s): 73.63.Kv, 73.23.Hk, 74.45.+c, 74.50.+r

Recently the fabrication of single quantum dots (QDs) coupled to superconducting leads has allowed study of the interplay between the Kondo effect and superconductivity in a gate tunable system.[1–7] While the QD Josephson junction has been studied in many systems,[1–4,7,8] hybrid normal-QD-superconductor (N-QD-S) devices have only been tackled in a few experimental studies[9–12] despite a wide range of theoretical treatments.[13–16] The N-QD-S system allows study of the interplay between Kondo effect and superconducting proximity effect from a new standpoint using a system with transport dominated by single Andreev reflection from which the local energy spectrum may be more easily deduced, in contrast to the complex multiple Andreev reflections which dominate in the superconductor-QD-superconductor (S-QD-S) system.[17] In a previous report[9] we used a weakly coupled N lead to probe Andreev energy levels formed with a strongly coupled S lead and studied the competition between superconducting pairing and electron-electron interactions. In the present study we focus on less asymmetrically coupled devices and observe that the Kondo singlet state may, for appropriate tunnel coupling with normal and superconducting leads, enhance the Andreev transport.

The Kondo effect arises at low temperatures when a localized unpaired electron spin is screened by delocalized conduction electrons and manifests as a dynamical singlet state, universally characterized by the Kondo temperature T_K. In a BCS s-wave superconductor electrons condense into a singlet state characterized by the superconducting energy gap Δ. In the S-QD-S system Kondo screening requires the breaking of Cooper pairs and is therefore in competition with the superconducting pairing. In this case a universal quantum phase transition is predicted in the system ground state from a BCS-like singlet state to a Kondo-like singlet state when $k_B T_K/\Delta \gtrsim 1$.[18–22] With finite coupling to a N lead the competition between proximity effect upon the QD and the N-lead Kondo screening must be considered.[14–16] The observation of the Kondo state in Andreev transport requires not only low temperature but also an appropriate tunnel coupling asymmetry between S and N leads.[16] The tunnel coupling asymmetry ($\chi=\Gamma_S/\Gamma_N$ in the S state) is determined from tunnel rates with the S lead ($\Gamma_S/\hbar$) and N lead ($\Gamma_N/\hbar$) which indicate the influence of single-particle processes and Andreev (coherent two-particle) processes, respectively. In one limiting case for $\Gamma_S \ll \Gamma_N$ the Kondo state is formed in the local density of states, at temperatures below the Kondo temperature (T_K^S for the system in the S state), but the corresponding resonance in Andreev transport is strongly suppressed as the S lead is effectively decoupled [Fig. 1(a)]. While in the limit $\Gamma_S \gg \Gamma_N$ particle-hole mixing induced by strong proximity effect drives the QD into a mixed-valence regime and the Kondo effect itself is suppressed. Strong particle-hole hybridization of the discrete QD energy levels results in a pair of Andreev energy levels in the single-particle energy spectrum[9] [Fig. 1(b)]. These indicate excitation between system ground state and excited state through the addition of an electron or hole at energy E_b relative to the Fermi energy. In the absence of Kondo screening the system ground state and excited state

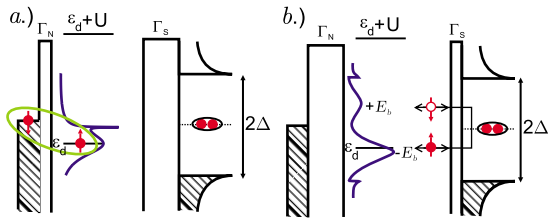

FIG. 1. (Color online) Schematics of the QD single-particle energy spectrum in limiting cases based on the tunnel coupling asymmetry. (a) If $\Gamma_S \ll \Gamma_N$ the Kondo effect dominates but low S-lead coupling limits the Andreev transport. (b) If $\Gamma_S \gg \Gamma_N$ strong proximity effect suppresses the Kondo state. Andreev energy levels at $\pm E_b$ dominate. In both schematics the bare QD energy level (ε_d) is drawn slightly below the fermi energy.

TABLE I. Relevant parameters for the regions considered. All values are estimated for the center of the odd electron occupation region. Note that χ for α-I exceeds the prediction in reference 9 due to the different method used.

	U (meV)	χ	T_K^N (K)	Γ (meV)	$\lvert g^* \rvert$
α-I	1.9	0.045	1.1 ± 0.2	~ 0.9	7.7 ± 0.1
α-III	2.0	25	1.2 ± 0.2	~ 0.9	5.4 ± 0.2
α-IV	2.0	8.0	1.2 ± 0.5	~ 1.0	5.5 ± 0.2
γ-IV	2.4	8.0	2.8 ± 0.3	~ 1.5	7.6 ± 0.4

can be either a degenerate, so-called "magnetic" doublet or BCS-like singlet or vice versa depending on the specifics of the bare QD energy level ε_d, charging energy U, Δ, and Γ_S. As the system is not fully gapped due to finite coupling with the N lead the Andreev energy levels have a width of $\sim\Gamma_N$ and are only well resolved if $\Gamma_N < \Delta$ and Γ.

Measurements are performed on single uncapped self-assembled InAs QDs contacted with one normal (Ti 10 nm /Au 50 nm) and one superconducting (Ti 5 nm /Al 150 nm) lead. The fabrication method is discussed elsewhere.[9] All measurements were performed in a He^3-He^4 dilution refrigerator ($T_{base} \sim 30$ mK) with conventional lock-in measurement techniques ($V_{ac} \sim 3\mu$ V). We measure a wide range of transport regions with typical $U \sim 1-3$ meV and energy-level spacings in the range $\Delta\varepsilon \sim 2-8$ meV. The tunnel coupling with the leads is determined by the overlap of the confined electron wave function with that of conduction electrons in the leads and is highly sensitive to the specific orbital state occupied.[23] In a single device a range of tunnel couplings may therefore be accessed simply by changing the charge state. Using two devices (labeled α and γ) we study four different odd electron occupation regions with parameters as summarized in Table I. The labels used to identify the device and roman numerals indicating regions with an odd electron occupation number are maintained from a previous publication[9] for continuity. Note that the roman numerals are used for convenience and do not denote the number of electrons occupying the QD, which we estimate to be a few tens.

Devices are characterized in the N state by applying an in-plane magnetic field greater than the Al lead critical field ($B_c \sim 220$ mT). An example of an N state charge stability diagram is plotted in Fig. 2(a) for region α-III, where we estimate $U \sim 2.0$ meV. In the N state the zero-bias conductance at the symmetry point (center of the odd occupation region) may be expressed as[24] $G_N = (2e^2/h)[(4\chi)/(1+\chi)^2]$. While estimates of χ are easily extracted, estimates of the total tunnel coupling are nontrivial. From the width of N-state Coulomb peaks we crudely estimate the total tunnel rate on/off of the QD $\Gamma = \Gamma_S + \Gamma_N$.

Figure 2(b) shows $G(V_{sd}, V_G)$ in the S state ($B = 0$ T). With one lead in the S state the key transport processes at low bias are Andreev reflections in which electron-hole pairs in the QD are converted to Cooper pairs in the S lead and vice versa. Such Andreev transport processes dominate all transport within the subgap region where $\lvert eV_{sd} \rvert < \Delta$. In the

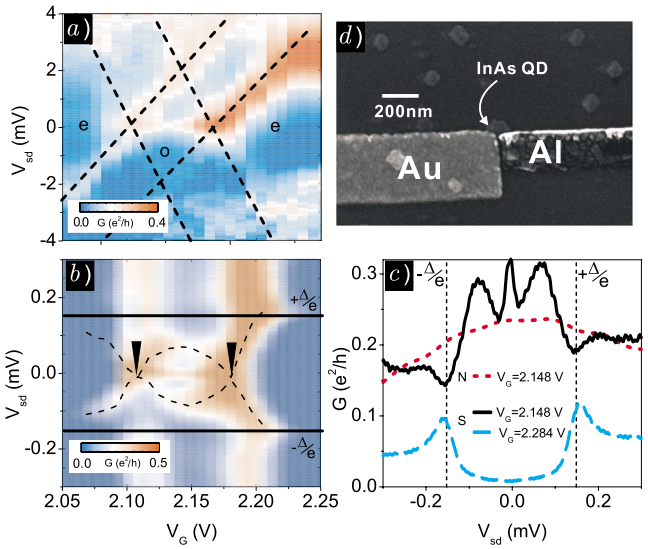

FIG. 2. (Color online) (a) Plots of differential conductance ($G = dI/dV_{sd}$) in the N-state ($B = 220$ mT) for region α-III. Even (e) and odd (o) electron occupation regions are indicated. (b) Plot of $G(V_{sd}, V_G)$ in the S state ($B = 0$ mT). Solid horizontal lines indicate the subgap region and dashed lines indicate Andreev energy-level resonances. Black arrows indicate points at which the Andreev energy levels cross. (c) $G(V_{sd})$ traces at the center of the odd electron occupation region in the N and S states and Coulomb blockade regime in the S state. (d) Scanning electron micrograph of device α.

even electron occupation regions, where energy levels are far from the superconducting gap and Coulomb blockade dominates, the subgap Andreev transport is strongly suppressed and the junction behaves as a conventional N-S tunnel junction in the weak tunneling limit[25] [Fig. 2(c)]. Here prominent transport resonances are attributed to single quasiparticle tunneling which is resonant with the high density of states at the edge of the superconducting energy gap when $\lvert eV_{sd} \rvert \sim \Delta$. From such features observed far from resonances with the discrete QD energy levels we estimate $\Delta \sim 152$ μeV, which corresponds with a temperature of $T \sim 1.76$ K. The superconducting transition temperature T_c is evaluated using $\Delta = 1.76 k_B T_c$ indicating $T_c \sim 1$ K.

In the odd electron occupation region a pair of subgap transport features which are symmetric in V_{sd}, [dashed lines in Fig. 2(b)] are attributed to the spectrum of Andreev energy levels on the QD,[26] providing clear evidence of strong proximity effect. Andreev reflection requires electron-hole pairs such that both Andreev energy levels [pictured in Fig. 1(b)] are probed in Andreev transport. In a previous report[9] with weakly coupled N-lead devices (where $\Gamma_N \ll \Gamma_S$ and the Kondo effect is suppressed) it was shown that the crossing of subgap Andreev transport resonances indicated the position of a phase transition between the BCS-like singlet and magnetic doublet ground states.[27] Following this phase transition the excited state (singlet or doublet) of the new phase is the ground state (doublet or singlet) of the previous and vice versa. In region α-III the subgap Andreev transport resonances cross at points indicated with black triangles in Fig. 2(b). Following the crossing the subgap transport displays a three-peak structure [Fig. 2(c)] with suppressed transport at

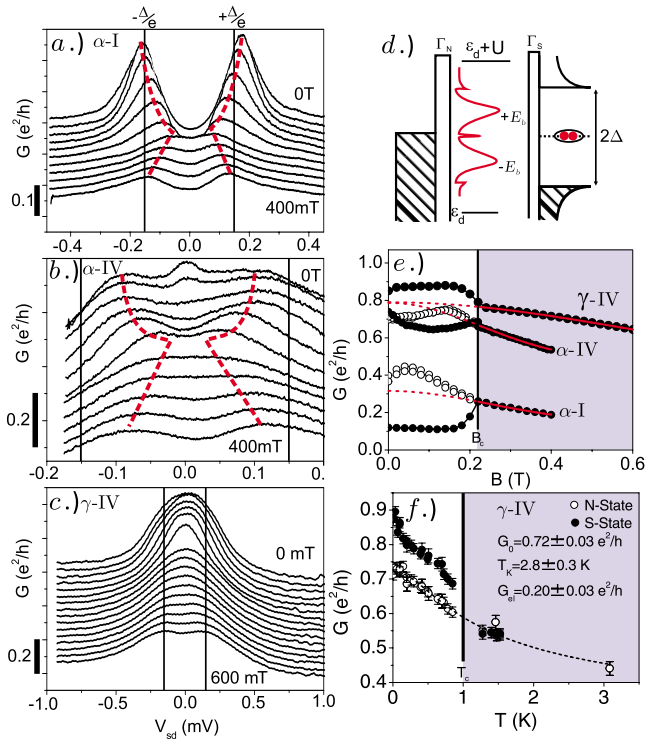

FIG. 3. (Color online) Plots of $G(V_{sd})$ for a range of B in the center of three odd occupation regions (a)α-I, (b) α-IV, and (c)γ-IV. Note that the V_{sd} scales are different and that curves are offset for clarity. (d) Schematic of the symmetrically coupled device at the symmetry point with $V_{sd}=0$ V showing Andreev energy levels at $\pm E_b$ and Kondo singlet state at the Fermi energy. (e) Plot of zero-bias conductance (●) and resonance conductance (○) as a function of B field. Solid lines indicate fitting for $B>B_c$ used to extract the $B=0$ mT N-state conductance. (f) Plot of extracted zero-bias N-state conductance (○) and S-state conductance (●) in region γ-IV.

the edge of the superconducting gap [Fig. 2(c)]. Simulations of the noninteracting N-QD-S system with a QD energy level within the superconducting energy gap[32,33] reveal that in the limit $\Gamma_S \gg \Gamma_N$ Andreev energy-level transport resonances are prominent while features are $|eV_{sd}| \sim \Delta$ are suppressed due to strong hybridization. The zero-bias conductance peak is consistent with Andreev transport enhanced by the Kondo singlet state in the local QD energy spectrum[16] [shown schematically in Fig. 3(d)] and the crossing Andreev energy-level resonances therefore indicates a crossover between BCS singlet state and Kondo singlet state[15] as the magnetic doublet is screened through Kondo processes. We note that the feature exhibits excellent qualitative agreement with a recent theoretical treatment by Domanski *et al.*[16] in which the Andreev conductance peaks indicating the Kondo singlet feature and Andreev energy levels were predicted to coexist in the transport for appropriate parameters. The half width at half maximum (HWHM) (HWHM$=k_BT_K$) of the N-state Kondo zero-bias anomaly gives an indication of the N-state Kondo temperature T_K^N. In the S state the conductance from Andreev processes is roughly proportional to the convolution of electron and hole density of states and as such the Lorentzian Kondo peak in the local density of states may be approximated in Andreev transport conductance with a squared Lorentzian fit of the Kondo zero-bias anomaly to extract an estimate of T_K^S. We estimate $T_K^S/T_K^N \sim 0.065 \pm 0.01$ indicating a significant reduction of Kondo temperature when one lead undergoes a transition to the superconducting phase and its contributions to the Kondo screening are suppressed. The S state T_K is therefore expected to always be lower than that in the N state.[14]

For the remainder of this Rapid Communication we compare transport in three odd electron occupation regions[32] which all display Kondo effect in the N state but different behavior in the S-state transport due to variation in χ and Γ. The evolution of $G(V_{sd})$ for increasing B measured in the center of the three odd electron occupation regions is displayed in Figs. 3(a)–3(c). In Fig. 3(e) we plot zero-bias conductance (●) as a function of applied magnetic field for regions α-I, α-IV and γ-IV. For comparison we also plot the conductance of the additional transport resonances (○) at low $B<B_c$, that is the single quasiparticle tunneling ($|eV_{sd}| \sim \Delta$) and subgap Andreev energy-level feature ($|eV_{sd}| < \Delta$) for α-I and α-IV, respectively. χ has been extracted by fitting a Lorentzian expression to data for $B>B_c$ and extrapolating to $B=0$ mT to estimate the conductance in the N state. We also estimate T_K^N from the temperature dependence of the evaluated normal-state conductance using the conventional empirical function[28,29] $G(T)=G_0/[1+(2^{1/s}-1)(T/T_K^N)^2]^s+G_{el}$, where G_0 is the $T=0$ K conductance, $s=0.21$ for a spin-$\frac{1}{2}$ system and G_{el} is a correction to account for elastic cotunneling processes.[30] An example of such analysis is presented in Fig. 3(f) for region γ-IV.

First we consider region α-I [Fig. 3(a)] in which χ is relatively low and favors the N lead. Here subgap Andreev transport is strongly suppressed when $B<B_c$ and prominent single quasiparticle tunneling features are observed at $|eV_{sd}| \sim \Delta$. The observed resonances are consistent with expectations from simulation of the noninteracting system[32,33] in the limit $\Gamma_N \gg \Gamma_S$ for which Andreev energy-level transport resonances are suppressed while single quasiparticle tunneling features at $|eV_{sd}| \sim \Delta$ are prominent. As B is increased Δ decreases, shifting the single quasiparticle tunneling resonances to lower V_{sd}. For $B>B_c$ the system enters the N-state and a conventional Kondo zero-bias anomaly which is split through the Zeeman effect is observed. Dashed lines in Fig. 3(a) indicate the evolution of the quasi-particle tunneling features to the Zeeman split Kondo feature. From the splitting of the Kondo zero-bias anomaly ($\Delta E=2|g^*|\mu_B$B, where g^* is the Landé g factor and μ_B the Bohr magneton) we estimate $|g^*|$ as summarized in Table I. It is likely that in region α-I the Kondo singlet state formed by N-lead screening is present in the local density of states, as T_K^N is high and the N-lead coupling dominates, but that the low S-lead tunnel coupling precludes observation of the Kondo feature in the Andreev transport. Note that the Andreev tunneling rate with the S lead will be reduced relative to the single-particle tunneling in the N state due to the strong electron-electron interaction.[15] In contrast to region α-I the other regions considered in this report have nominally dominant S-lead coupling and display pronounced subgap Andreev transport resonances in the S state.

For low B in region α-IV [Fig. 3(b)] we observe a pair of Andreev energy-level transport resonances and a narrow zero-bias peak which we attribute to Kondo-enhanced Andreev transport. The reduction of Δ with increasing B shifts the Andreev energy-level transport resonances to lower V_{sd} until $B > B_c$ where Zeeman split Kondo features are observed. In Fig. 3(b) the dashed line indicates the evolution of Andreev energy-level resonances to Zeeman split Kondo features. The rapid suppression of the zero-bias peak as B is increased indicates a small T_K^S which is quickly exceeded by the Zeeman splitting. Compared with region α-III discussed earlier (Fig. 2) we find that Andreev energy-level resonances are poorly resolved in region α-IV which we may attribute to the stronger Γ_N (smaller χ) which results in broader features in the local energy spectrum. Graber *et al.*[10] investigated a N-QD-S device fabricated using a multiwalled carbon nanotube QD and observed a Kondo zero-bias anomaly in the Andreev transport when $k_B T_K^N > \Delta$. In the present study we observe Kondo-enhanced transport in regions α-III/α-IV even for $k_B T_K^N < \Delta$. Our results display good qualitative agreement with theoretical treatments[14–16] which predict Kondo-enhanced transport only for χ close to unity.

Finally, the effects of very large Γ may be observed in region γ-IV [Fig. 3(c)] in which $k_B T_K^N$ significantly exceeds Δ. Here a single broad conductance peak is observed in the S state with a clear enhancement of the zero-bias conductance at the N-S phase transition [Figs. 3(e) and 3(f)]. Features indicating the Andreev energy levels are unclear, but the broad conductance peak is observed to narrow as B is increased, contrary to behavior expected of a Zeeman split Kondo zero-bias anomaly. We attribute this behavior to the presence of broad subgap Andreev energy levels which are shifted toward the Fermi energy with increasing B (decreasing Δ). Here the large Γ_N does not allow the Andreev energy levels to be resolved in transport. High T_K^N indicates that the S lead may also contribute to screening the localized spin. Theoretical treatments of the QD-S system for $k_B T_K > \Delta$ indicate that the Kondo singlet state feature in the local density of states is enhanced at the expense of subgap Andreev energy levels[27,31] which may also affect the visibility of these features in region γ-IV.

The authors thank A. Oguri and Y. Yamada for fruitful discussions and acknowledge financial support from the Japan Society for the Promotion of Science, Grant No. P07328 (R.S.D.), Special Researchers Program of RIKEN (Y.T.), and Grant-in-Aid for Scientific Research S (Grant No. 19104007) and B (Grant No. 18340081).

*russell@meso.t.u-tokyo.ac.jp

[1] M. Buitelaar *et al.*, Phys. Rev. Lett. **89**, 256801 (2002).
[2] T. Sand-Jespersen *et al.*, Phys. Rev. Lett. **99**, 126603 (2007).
[3] A. Eichler *et al.*, Phys. Rev. Lett. **99**, 126602 (2007).
[4] J. Cleuziou *et al.*, Nat. Nanotechnol. **1**, 53 (2006).
[5] A. Eichler *et al.*, Phys. Rev. B **79**, 161407(R) (2009).
[6] C. Buizert *et al.*, Phys. Rev. Lett. **99**, 136806 (2007).
[7] P. Jarillo-Herrero, J. van Dam, and L. Kouwenhoven, Nature (London) **439**, 953 (2006).
[8] J. van Dam *et al.*, Nature (London) **442**, 667 (2006).
[9] R. Deacon *et al.*, Phys. Rev. Lett. **104**, 076805 (2010).
[10] M. Gräber *et al.*, Nanotechnology **15**, S479 (2004).
[11] L. Hofstetter *et al.*, Nature (London) **461**, 960 (2009).
[12] L. G. Herrmann *et al.*, Phys. Rev. Lett. **104**, 026801 (2010).
[13] R. Fazio and R. Raimondi, Phys. Rev. Lett. **80**, 2913 (1998); Phys. Rev. Lett. **82**, 4950 (1999).
[14] J. Cuevas, A. L. Yeyati, and A. Martin-Rodero, Phys. Rev. B **63**, 094515 (2001).
[15] Yoichi Tanaka, N. Kawakami, and A. Oguri, J. Phys. Soc. Jpn. **76**, 074701 (2007).
[16] T. Domanski and A. Donabidowicz, Phys. Rev. B **78**, 073105 (2008); **76**, 104514 (2007).
[17] M. Buitelaar *et al.*, Phys. Rev. Lett. **91**, 057005 (2003).
[18] L. Glazman and K. Matveev, Sov. Phys. JETP **49**, 659 (1989).
[19] M.-S. Choi *et al.*, Phys. Rev. B **70**, 020502(R) (2004).
[20] F. Siano and R. Egger, Phys. Rev. Lett. **93**, 047002 (2004); **94**, 039902 (2005).
[21] C. Karrasch, A. Oguri, and V. Meden, Phys. Rev. B **77**, 024517 (2008).
[22] Yoshihide Tanaka, A. Oguri, and A. C. Hewson, New J. Phys. **9**, 115 (2007).
[23] M. Jung *et al.*, Appl. Phys. Lett. **87**, 203109 (2005).
[24] S. Hershfield, J. Davier, and J. Wilkins, Phys. Rev. Lett. **67**, 3720 (1991).
[25] G. Blonder, M. Tinkham, and T. Klapwijk, Phys. Rev. B **25**, 4515 (1982).
[26] M. Governale, M. Pala, and J. König, Phys. Rev. B **77**, 134513 (2008).
[27] J. Bauer, A. Oguri, and A. Henson, J. Phys.: Condens. Matter **19**, 486211 (2007).
[28] T. K. Ng and P. A. Lee, Phys. Rev. Lett. **61**, 1768 (1988).
[29] L. Glazman and M. E. Raikh, JETP Lett. **47**, 281 (1988).
[30] M. Pustilnik and L. I. Glazman, Phys. Rev. Lett. **87**, 216601 (2001).
[31] M. Krawiec and K. Wyokinski, Supercond. Sci. Technol. **17**, 103 (2004).
[32] See supplementary material at http://link.aps.org/supplemental/10.1103/PhysRevB.81.121308 for additional device characterization details and simulations of the noninteracting system.
[33] V. Khlus, A. Dyomin, and A. Zazunov, Physica C **214**, 413 (1993).